Citation: BoneKEy Reports **1,** Article number: 37 (2012) | doi:10.1038/bonekey.2012.28

www.nature.com/bonekey

REVIEW

Advances in multimodality molecular imaging of bone structure and function

Floor M Lambers, Gisela Kuhn and Ralph Müller

Institute for Biomechanics, ETH Zurich, Zurich, Switzerland.

The skeleton is important to the body as a source of minerals and blood cells and provides a structural framework for strength, mobility and the protection of organs. Bone diseases and disorders can have deteriorating effects on the skeleton, but the biological processes underlying anatomical changes in bone diseases occurring *in vivo* are not well understood, mostly due to the lack of appropriate analysis techniques. Therefore, there is ongoing research in the development of novel *in vivo* imaging techniques and molecular markers that might help to gain more knowledge of these pathological pathways in animal models and patients. This perspective provides an overview of the latest developments in molecular imaging applied to bone. It emphasizes that multimodality imaging, the combination of multiple imaging techniques encompassing different image modalities, enhances the interpretability of data, and is imperative for the understanding of the biological processes and the associated changes in bone structure and function relationships *in vivo*.

BoneKEy Reports **1**, Article number: 37 (2012) | doi:10.1038/bonekey.2012.28

Introduction

Bone tissue continuously remodels to repair microcracks, prevent the accumulation of microdamage,[1] adapt to local stresses[2] and maintain calcium homeostasis in the blood.[3] In many bone diseases, bone remodeling is disturbed; that is, bone formation (governed by osteoblasts) and bone resorption (governed by osteoclasts) are unbalanced, resulting in altered mechanical properties of the bone. Clinical diagnosis of bone diseases typically relies on detection of bone mineral density or bone microstructure measured with anatomical imaging techniques such as dual-energy X-ray absorptiometry or peripheral quantitative computed tomography (CT).[4,5] Currently available imaging techniques are not adequate for detecting bone diseases at a stage early enough to prevent deterioration of the bone microstructure, because factors like genetic background, hormones, cytokines and mechanical stimuli, have an important influence on bone remodeling, but are difficult to measure and visualize and are therefore not easily accessible to quantitative assessment *in vivo*.[6,7] Furthermore, anatomical imaging will typically detect a disease at a later stage of the disease progression, as it will manifest itself only once changes in bone mass or structure are apparent, whereas changes in bone metabolic activity will precede these anatomical changes,[8,9] and with that, offer a more sensitive avenue for early diagnosis, but also in response to therapy. Therefore, *in vivo* evaluation of bone metabolic activity would allow earlier and more reliable diagnosis of bone diseases and improved monitoring of therapy and intervention.

Molecular imaging is such a technique, enabling non-invasive characterization, quantification and visualization of biological processes *in vivo* at the cellular and molecular level.[10] The Society of Nuclear Medicine defines molecular imaging as 'the visualization, characterization and measurement of biological processes at the molecular and cellular levels' in living systems. Thus, as biological processes can be monitored over time and a fast non-destructive read-out is provided, molecular imaging leads to a more fundamental understanding of the *in vivo* progression of diseases and allows assessment of the effectiveness of treatment and new classes of drugs.[11,12] Nevertheless, a general limitation of molecular imaging is the low spatial resolution that is inherent to all molecular imaging approaches. Therefore, to obtain a full understanding of how bone remodeling is influenced by bone diseases, there is a need for combined molecular and anatomical imaging, which typically defines the combination of different imaging modalities to create a 'fused' image-visualizing signals from different imaging sources, an approach also termed multimodality imaging.

Correspondence: Professor Dr R Müller, Institute for Biomechanics, ETH Zurich, Wolfgang-Pauli-Strasse 10, HCI E357.2, Zurich 8093, Switzerland.
E-mail: ram@ethz.ch

Received 13 November 2011; accepted 17 January 2012; published online 22 February 2012

In this perspective, the latest developments in molecular imaging in bone research are reviewed with emphasis on the importance of multimodality imaging. First, the latest developments in molecular imaging and multimodality systems are provided. Second, methods available for dynamic imaging of bone remodeling will be introduced. Third, several areas of bone research are explored for the application of multimodality molecular imaging. The focus will be on multimodality molecular imaging in pre-clinical *in vivo* animal models of bone disease and therapy.

Molecular Imaging Modalities

Two main molecular imaging methods are available for applications in bone: nuclear imaging (ionizing) and optical imaging (non-ionizing). For nuclear imaging, radiopharmaceuticals, consisting of a radionuclide bound to a reporter construct that allows binding of the probe to a biological signal of interest, are administrated. Radiopharmaceuticals that emit single gamma rays can be detected by bone scintigraphy and single photon emission CT (SPECT), allowing detection of a biological signal of interest. For SPECT, multiple projections are captured providing a three-dimensional image. Similarly, positron emission tomography (PET) is based on the coincidence detection of two gamma rays that formed through the annihilation of positrons emitting from the radionuclide and electrons in the host tissue, allowing localizing biological signals of interest.[13]

Optical imaging techniques rely on the detection of photons and include near-infrared fluorescence imaging, fluorescence molecular tomography (FMT) and bioluminescence imaging (BLI). For near-infrared fluorescence imaging and FMT, fluorophores, consisting of a fluorochrome bound to a reporter construct that allows binding of the probe to a biological signal of interest, are administrated. When the fluorochrome is excited by laser diodes, it emits light at a different frequency in the near-infrared range (700–900 nm), which can be detected with a charge-coupled device camera,[14] allowing detection of a biological signal of interest. For FMT, multiple projections are captured building up a three-dimensional image.[15] For

Table 1 Overview of imaging strategies in bone research

Nuclear imaging: Relies on pharmaceuticals that have been labeled with radionuclides

Imaging modality	Probe	Description
Bone scintigraphy/SPECT	^{99m}Tc-MDP	Targets the calcium in hydroxyapatite.[33]
PET	^{18}F-fluoride	Targets the hydroxyl groups in hydroxyapatite.[34]
	^{18}F-FDG	An indicator of cellular glucose metabolism.[77]

Optical imaging: Relies on the detection of photons from exogenous fluorochromes (linked to biological response)

Imaging modality	Probe	Description
NIRF/FMT	OsteoSense	A bisphosphonate (pamidronate) bound to a near-infrared (NIR) fluorophore (IRDye78). Targets hydroxyapatite.[43]
	Indocyanine green-alendronate conjugate	A bisphosphonate (alendronate) bound to a NIR fluorophore (indocyanine green). Targets hydroxyapatite.[45]
	BoneTag (LI-COR Biosciences, Lincoln, NE, USA)	A tetracycline derivative bound to a NIR fluorophore (IRDye 800CW). Targets hydroxyapatite.[46]
	Cathepsin-K	Targets cathepsin-K, which is expressed in active osteoclasts and involved in the breakdown of the bone matrix.[8]
BLI	OC (hOC promoter)	Targets osteocalcin, which is expressed by osteoblasts and involved in tissue mineralization.[49]
	Firefly luciferase coupled to MSCs	Targets stem cells that have the capacity to differentiate into osteoblasts and proliferate.[51]

Anatomical imaging:

Imaging modality	Feature	Description
In vivo micro-CT	Anatomical changes in bone microstructure	By using serial images, locations of bone formation and bone resorption can be visualized and morphometrically described.[55]
MRI	Bone marrow	The trabecular bone marrow can be resolved from the relaxation rate, and the trabecular bone volume fraction from the attenuation of the spin-echo amplitude.[78]

Abbreviations: BLI, bioluminescence; CT, computed tomography; FDG, fluorodeoxyglucose; FMT, fluorescence molecular tomography; hOC, human osteocalcin; MDP, methylenediphosphonate; MSCs, mesenchymal stem cells; MRI, magnetic resonance imaging; NIRF, near-infrared fluorescence; PET, positron emission tomography; SPECT, single photon emission CT.

BLI, mice are genetically modified to express luciferase simultaneously with a gene of interest. Upon injection of luciferin, light is emitted from the gene of interest.[16] An overview of the available imaging strategies that make use of molecular probes for *in vivo* assessment of dynamic bone remodeling is shown in **Table 1**.

Anatomical Imaging Modalities

Imaging modalities that allow for anatomical imaging of bone include CT and magnetic resonance imaging (MRI). Contrast for CT depends on the linear attenuation coefficients of all the structures through which the X-ray beam passes.[17] Multiple projections are performed to form a three-dimensional image with a resolution reaching up to 10 μm for rodents and 40 μm for humans.

MRI is based on the resonance of protons in atomic nuclei. In a strong magnetic field, the protons of the nuclei in the tissue align. When this equilibrium is disturbed by a radiofrequency pulse, magnetization is recovered with a tissue-specific relaxation time, providing the basis for contrast.[18] By repeated radiofrequency pulses, a three-dimensional image with a resolution on the order of 100 μm can be build up from a stack of cross-sectional images.

Multimodality Systems

Multimodality imaging allows integration of molecular (functional) with anatomical (structural) information, offering the benefits of each single imaging modality, and at the same time, eliminate one or more inadequacies of the individual modality.[19] Multimodality imaging systems therefore allow the combination of high sensitivity, high specificity and high spatial resolution.

Basically, there are two different ways of multimodality imaging, one in which multiple imaging modalities are merged into one system (multimodality scanners), and another in which, after imaging on multiple imaging systems, the images are registered and fused (software approach).[20] Multimodality scanners can acquire functional and structural images without moving the subject from the bed, as the hardware of both imaging systems is combined. These scanners thus provide the most precise fusion of images and enable a more specific diagnosis, but have a complicated design that often involves compromising the image quality, and they are also very expensive.[21] The most commonly used multimodality scanners in clinical practice are PET/CT[22] and SPECT/CT.[23] Multimodality scanners that combine PET/MRI,[24] PET/optical imaging,[25] FMT/CT[26] and FMT/MRI[27] have been developed as well and are mostly confined to preclinical research.

The second form of multimodality imaging often uses one bed to transport the subject between modalities, and needs registration algorithms to ensure correct alignment between imaging modalities and to allow superimposition of images from different modalities.[28] Rigid registration rotates and translates images between modalities, and can only be used correctly when no movement of the subject occurred between modalities.[9] With subject motion, non-rigid registration techniques have to be used, which allow deformation or scaling of the images from the different imaging sources. Non-rigid registration is mathematically more complicated and typically very demanding computationally.[29] An imaging chamber or bed that rigidly fixes the subject together with fiducial markers visible in all modalities will improve registration and therefore allow more accurate image fusion;[30] however, involuntary movement and changes in the shape of organs remain complications.[23]

Time-Lapsed Imaging of Bone Remodeling Activity

During new bone formation, osteoid becomes increasingly mineralized through crystallization of hydroxyapatite ($Ca_{10}(PO_4)_6OH_2$) by osteoblasts. Therefore, substances that bind to bone mineral can be used as markers for bone formation or newly opened surfaces due to damage and microcracking. Bisphosphonates are a group of commonly used substances which naturally display a high affinity for bone mineral and bind to the calcium in hydroxyapatite through the phosphonate–carbon–phosphonate moiety, or to the hydroxyl group in hydroxyapatite through the nitrogen moiety.[31] This process opens opportunities to use these substances to bring molecular imaging probes to the bone surfaces and use these probes for time-lapsed imaging of bone activity, targeting osteoblastic formation, osteoclastic resorption, or even both at the same time.

In bone scintigraphy and SPECT, ^{99m}Tc-methylenediphosphonate (MDP) which is a radionuclide tracer linked to a bisphosphonate, is used to evaluate bone metabolic activity.[32] Incorporation of ^{99m}Tc-MDP can be related to the exchange of phosphorous groups with the calcium of crystallizing hydroxyapatite,[33] and can thus be used as a measure of activity of new bone formation.

In PET, ^{18}F-fluoride is used as a radiotracer targeting hydroxyapatite. Hydroxyl groups in the hydroxyapatite crystal of bone ($Ca_{10}(PO_4)_6OH_2$) are replaced by fluoride ions, resulting in fluoroapatite ($Ca_{10}(PO_4)_6F_2$).[34] ^{18}F-fluoride has been shown to deposit preferentially at the surface of bone, where the greatest activity of remodeling and turnover is seen.[35,36] The marker can provide quantitative estimates of bone cell activity,[37] and has allowed assessment of fracture healing[38] or implant ingrowth after hip surgery.[39,40] ^{18}F-fluoride–PET is quantitatively more precise than ^{99m}Tc-MDP SPECT,[41,42] because of the higher resolution and improved calibration in PET imaging.

In near-infrared fluorescence imaging, OsteoSense (PerkinElmer, Boston, MA, USA) is used as a marker to measure local bone metabolism. This probe consists of a bisphosphonate (pamidronate) and a fluorophore (IRDye78, LI-COR Biosciences) and binds with great affinity to mineralizing bone surfaces.[43,44] Near-infrared fluorescence imaging, in combination with OsteoSense-labeling, has been shown to provide improved resolution and sensitivity compared with ^{99m}Tc-MDP SPECT[33] in small animals. Besides OsteoSense, other such conjugates were recently developed consisting of a bisphosphonate and a fluorophore, for example, a probe with alendronate and indocyanine green, which binds to metabolically active areas in the bone and remains visible in the body for 2 weeks.[45] Tetracycline is another compound targeted at hydroxyapatite, which has been around for decades and is still often used in histomorphometry to demarcate positions of new bone formation and to calculate changes in bone formation rates. Using the same concept as with the bisphosphonate-based probes, a tetracycline derivative bound to a fluorophore (IRDye 800CW, LI-COR Biosciences) was recently introduced to image sites of bone remodeling *in vivo*, using an optical imaging approach.[46] What is interesting about these approaches is that all of these probes are excited at different wave lengths (e.g., green or red),

and therefore, can be targeted to visualize different effects and/or different time points *in vivo* in a single subject by tuning the filter of the fluorescence detector.

Besides the affinity to hydroxyapatite, other approaches have used different bone proteins as the direct target for the molecular probe. Osteocalcin is such a bone matrix protein, which is expressed by osteoblasts, odontoblasts and hypertrophic chondrocytes at the onset of tissue mineralization.[47] Although the exact function of osteocalcin is unclear, it is assumed to have an important role in mineral deposition, bone remodeling and bone mineral maturation,[48] and with that, is interesting as molecular target. Using this concept, transgenic mice expressing a luciferase reporter gene under regulation of the human osteocalcin promoter were used to monitor the calcein gene expression with BLI as yet another marker for changes in bone formation.[49,50] In another approach, human bone marrow mesenchymal stem cells (MSCs) were transfected with firefly luciferase to monitor the survival and proliferation of human bone marrow MSCs. As human bone marrow MSCs have the capacity to differentiate into osteoblasts,[51] this approach allows to investigate autologous bone repair and precise quantification of bone metastatic growth *in vivo*.[52,53]

Although there are a number of molecular probes targeting bone formation, only one probe is available that targets osteoclast using a cathepsin K-activatable near-infrared fluorescence probe. In the presence of cathepsin K, side groups which are otherwise quenched are cleaved off from the probe and emit fluorescence.[54] The cathepsin K probe is sensitive to changes in bone resorption and has been shown to precede detection of bone loss, using anatomical imaging systems.[8]

Although the use of molecular probes is very sensitive, there is still always the problem of low resolution in these systems, making it sometimes difficult to assign bone function to a specific structure. Recently, a new method was developed that allows monitoring sites of bone formation and bone resorption from time-lapsed *in vivo* micro-CT images[55] using unprecedented resolution. Nevertheless, this method allows monitoring longitudinal changes in bone formation and resorption rates induced by mechanical loading[56] and bone regeneration.[57]

Applications of Multimodality Molecular Imaging in Bone Research

Bone metastases. Bone metastases are a frequent complication of many common cancer types, occurring in about 80% of patients with breast, lung or prostate cancer,[58] and cause considerable pain.[59] Bone metastases are typically referred to as osteolytic when the main effect is bone destruction, and sclerotic when there is mainly increased osteoblastic activity.[60] ^{99m}TC-MDP bone scintigraphy is the most widely used method for evaluating skeletal metastases in humans.[61] Nevertheless, MRI and fluorodeoxyglucose (FDG)–PET/CT studies are far more sensitive for revealing metastases than bone scintigraphy.[62] When ^{18}F-FDG–PET and CT are concordant, this leads to a very high positive predictive value for bone metastases (98%). However, in metastases with discordant PET and CT findings, the positive predictive value is markedly diminished. Independently, the positive predictive value of all lesions is significantly higher with PET than with CT.[63] The distinction between benign and malignant lesions can usually be achieved by registration of ^{18}F-FDG–PET with CT.[64] Furthermore, ^{99m}Tc-MDP SPECT can differentiate between malignant and benign metastases when ^{99m}Tc-MDP SPECT and CT are registered,[23] indicating the importance of multimodality imaging.

In a recent study, the development, metabolism and progression of metastatic tumor formation in mice with induced lung tumors was characterized using small-animal PET imaging and *in vivo* micro-CT.[65] Mice were imaged with micro-CT every other day until tumors were anatomically identified, at which point ^{18}F-FDG–PET was performed in the same mouse holder. Small-animal PET imaging did not identify any metastases that were not previously detected by *in vivo* micro-CT. However, micro-CT was capable of detecting metastases that were not detected by small-animal PET, based on the resolution limits of the used instrumentation. The CT/PET fusion imaging correctly correlated radiotracer uptake with anatomical location, demonstrating the utility of multimodality imaging in oncology. However, only 36% of the tumors confirmed on histopathology were found with micro-CT, because for some tissues, the contrast of CT was not adequate for the identification of tumors, and for other tissues, the size of the tumors was too small.[65] In contrast to imaging with micro-CT until tumors are evident, in another study, PET was used until a bone metastasis was detected, from which time point on anatomical imaging was performed to locate the malignancy.[66] It was found that lesions smaller than 2.5 mm^3 are more reliably detected by micro-CT than by micro-PET, which shows that even though PET has a higher sensitivity, the limited resolution does not allow detection of small lesions. Sclerotic metastases, on the other hand, led to distinctly elevated bone turnover that was more easily detected and monitored on ^{18}F-fluoride–PET scans.[67]

BLI has also been used in research of bone metastases; BLI offers the important advantage of detecting tumor growth in the marrow cavity long before development of radiologically evident osteolytic and/or osteosclerotic lesions.[53] Mice with an intracardiac injection of cancer cells transfected with luciferase showed distinct areas of photon accumulation after 4 weeks in the distal metaphyses of femurs and dorsal side of thoracic vertebrae, suggestive of metastatic tumor growth, where osteolysis was not evident on radiographs. Also bone metastases caused by intraosseous implantation of cancer cells could be detected by BLI from 4 days after implantation onwards, although metastases were only evident with radiography from day 14 on (**Figure 1**).[53] Similarly, when tumor cells were injected into the bone marrow space, evidence of the presence of a bone lesion was detectable after 2 days with BLI and after 7 days only with micro-CT.[68]

Osteoporosis. A frequently used model for studying biological pathways underlying postmenopausal osteoporosis is the removal of ovaries in mice or rats (OVX) to induce estrogen deficiency. OVX mice showed a faster bone turnover than sham or bisphosphonate-treated OVX mice as determined by an increase in bone formation by OsteoSense–FMT, and an increase in osteoclast activity as measured with cathepsin-K–FMT. Osteoclast activity was evident at an earlier time point than bone loss detected with micro-CT.[8]

Cyclic loading response. Among other factors, bone remodeling is influenced by the micromechanical environment. To better understand how mechanical forces influence bone remodeling, animal models of load adaptation are often employed. In one study where changes in bone remodeling as well as changes in bone microstructure were monitored over time, it was

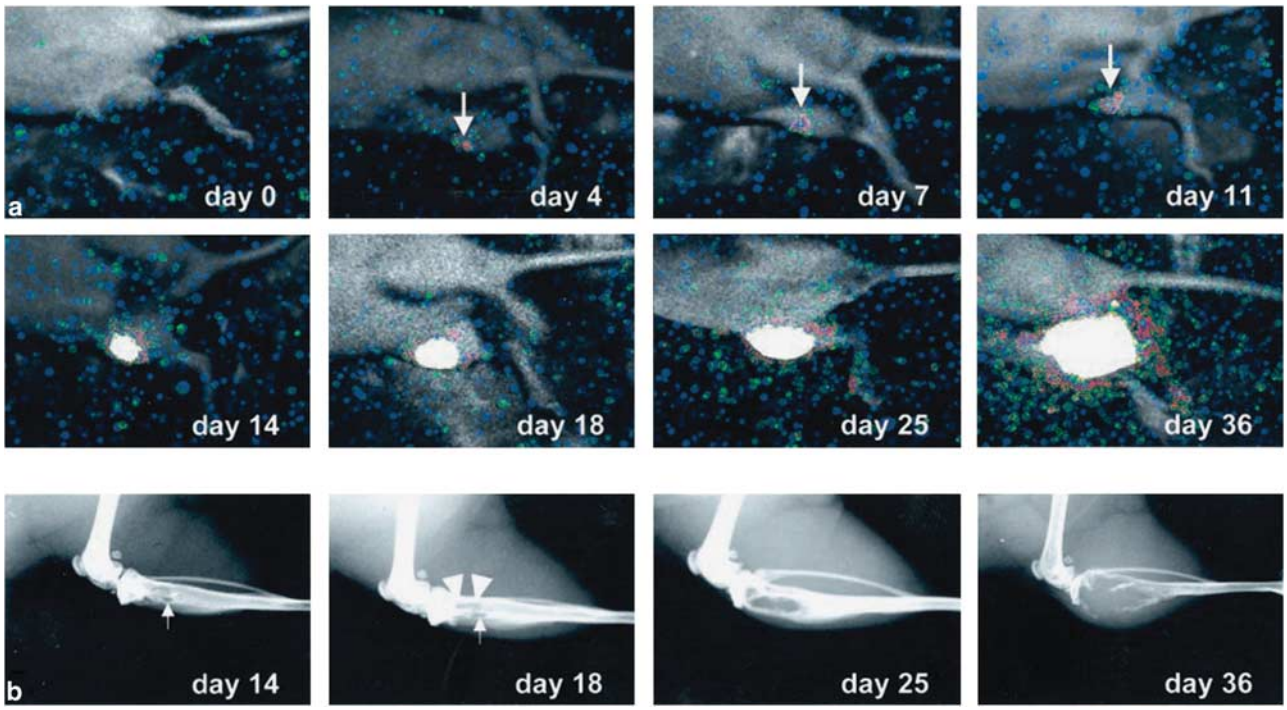

Figure 1 Monitoring of bone metastasis induced by implantation of cancer cells in the marrow cavity of the tibia. (**a**) With BLI, a signal at the site of implantation was detectable from day 4 on and became intense from day 14 on. (**b**) Radiologically, the metastasis showed an initial sign only at day 14. Reproduced with permission from Wetterwald *et al.*[53]

shown that 15-week-old mice responded to mechanical loading by increasing bone formation rate and decreasing bone resorption rate, leading to an increase in bone volume density. Changes in bone remodeling rates were mostly an effect of changes in the surface occupied and not thickness of remodeling sites, whereas the amount of remodeling sites was not different from control group, indicating that the osteoblast and osteoclast activity were modulated rather than the osteoblast and osteoclast number.[56] Although only one scanner was used in this study, it can be regarded as a multi-modality approach, because both anatomical and functional parameters were extracted.

Fatigue loading response. Another approach to initiate bone remodeling in animal models is to create microdamage through fatigue-impact loading. Rats that were subjected to a single bout of fatigue loading, consisting of displacements between 45 and 85% of the average displacement to complete fracture (2.0 mm), showed an increase in ^{18}F-fluoride uptake in the central portion of the loaded forelimb, which reduced with time after loading.[69] By registration of the PET and CT images (with the help of fiducial markers), the location of increased bone remodeling could be observed (**Figure 2**). In this case, CT only served as an anatomical reference for PET, because the resolution was not sufficient to analyze morphological changes in the cortical bone.[69]

Fracture healing. Five to ten percent of the fractures that occur annually in the United States demonstrate delayed healing or non-union.[70] Such fractures require multiple surgical procedures and are associated with disability, pain and prolonged rehabilitation periods.[71] To better understand processes underlying fracture healing, animal models have been used, in which defects or fractures are created in the bone or in which spacers are inserted to simulate non-union.[72] ^{18}F-fluoride uptake increased in a study, in which fractures were created in femurs of rats, whereas in rats with non-unions, minimal ^{18}F-fluoride uptake was found, indicating that ^{18}F-fluoride–PET could distinguish healing fractures from non-unions already 1 week after the operation and may have a role in the assessment of longitudinal fracture healing.[38] Similarly, on plain radiographs, it was also evident whether the bone was, or was not, healing from week 2 onwards; callus formation was visible in the fracture group, whereas no bone formation was visible in the non-union group.

Besides delayed- or non-unions, infections are a common complication of fracture healing. In rats, in which a bacterial infection was induced in a tibial defect, the feasibility of a new tracer, targeted at a protein that is only expressed at sites of inflammation, was evaluated. This novel PET-imaging agent allowed distinguishing bone infection and normal bone healing (which involves inflammation, but not infection) as soon as 1 week after surgery. At the same time point, cortical bone destruction was visible in infected bones with peripheral quantitative CT, whereas normal bone healing was observed in control rats, further confirming the applicability of the novel PET-imaging agent.[73]

To facilitate healing of complicated fractures, MSCs can be delivered to the site of injury. When homing of luciferase-transfected MSCs was analyzed in a defect in the femur of mice, a higher BLI signal was found in injected mice than in control mice, indicating attraction of MSCs to the injured tissue. No difference between mice injected with MSCs and a control group was found with ^{18}F-fluoride PET, likely due to the low number of MSCs in the region of interest, but for both groups, the fractured femur showed greater uptake than contralateral control. Furthermore, micro-CT measurements revealed accelerated bone healing in treated compared with control group. This indi-

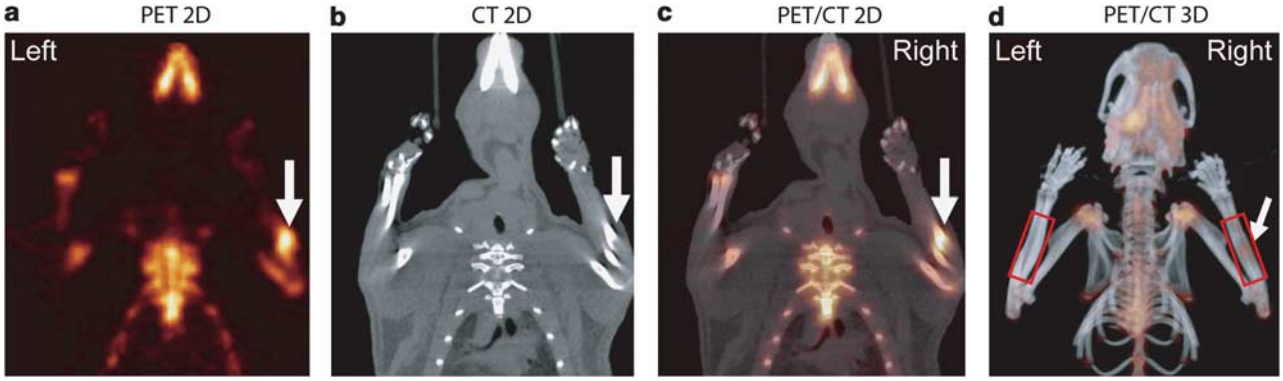

Figure 2 Single slice of PET (**a**), CT (**b**), registered slice (**c**) and co-registered PET/CT projection (**d**) image of the cranial half of a rat on day 4 after fatigue loading in the high displacement group. Symmetric ^{18}F-fluoride uptake was observed in regions of higher bone turnover. More ^{18}F-fluoride uptake was observed in the central region of the loaded forelimb (arrow) than in the unloaded forelimb. Reproduced with permission from Silva *et al.*[69]

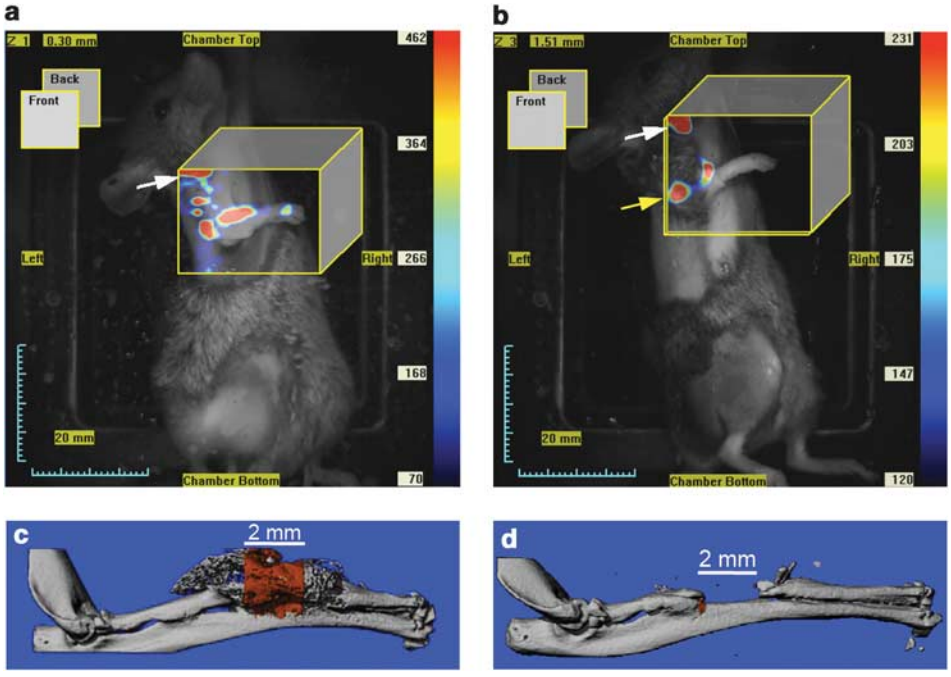

Figure 3 FMT images after 3 weeks (**a**, **b**) and micro-CT images (**c**, **d**) of group implanted with MSCs overexpressing BMP2 (**a**, **c**) and not overexpressing BMP2 (**b**, **d**). A greater fluorescence signal was observed in the group overexpressing BMP2 (**a**), and correspondingly new bone formation was shown in the radial defect (**c**). For the control group the fluorescence signal was lower (**b**) and almost no bone formation was found (**d**). Reproduced with permission from Zilberman *et al.*[75]

cated that MSCs promoted healing, which could only be verified through a multimodality approach.[74]

Bone morphogenic protein-2 (BMP2) is an osteoinductive protein that can induce bone formation *in vivo*. Therefore, MSCs overexpressing BMP2 (MSCs–BMP2) could enhance bone healing. Indeed, a significant OsteoSense signal was observed with FMT in mice with a non-union bone defect in the radius implanted with MSCs–BMP2, whereas little or no signal could be detected in mice injected with MSCs without BMP2 overexpression (**Figure 3**). In agreement, new mineral deposition as assessed with micro-CT had occurred in the non-union bone defect at 3 weeks in mice implanted with MSCs–BMP2, whereas in control mice, no bone formation was found.[75] Similarly, intervertebral discs injected with MSCs–BMP2 under a tetracycline-controlled expression system retained a high fluorescence signal up to 4 weeks post injection detected with BLI, and caused fusion of vertebral bodies as revealed with micro-CT.[76]

Discussion and Conclusion

In this review, recent advances in multimodality molecular imaging of bone structure and function were presented. Molecular imaging allows non-invasive monitoring of specific biological processes within living subjects and is complimentary to anatomical imaging. PET provides great sensitivity, but lacks spatial resolution and is associated with radiation dosage and radionuclide toxicity. Similarly, optical imaging has great sensitivity and temporal resolution, but lacks spatial resolution and sufficient penetration depth. By combining molecular with anatomical imaging, early changes in bone remodeling can be imaged and quantified. In the field of molecular imaging, considerable

progress has been made in the further development of imaging techniques and molecular probes over the past decade. These advances have led to a greater understanding of bone diseases and disorders.

Nuclear imaging techniques, including ^{18}F-fluoride–PET, ^{18}F-FDG–PET and ^{99m}Tc-MPD–SPECT or bone scintigraphy are regularly used in the clinics, whereas optical imaging techniques (FI and FMT) are often only performed in research, and BLI is currently limited to research in mice, due to the need of transgenic mice. The most important hurdle in translating optical imaging to clinical applications is the depth of penetration, which is on the order of one centimeter, therefore only allowing superficial measurements in larger animals or humans. A further difficulty for optical bone imaging is the need for fluorescent probes, which are unlikely to be approved for clinical use in humans. As a consequence, for bone imaging, PET/CT and SPECT/CT-multimodality scanners are widely used in the clinics, especially in the field of oncology, whereas other multimodality scanners are only used in research or preclinical settings. General limitations of multimodality scanners are the cost and the computational power needed for image registration and image fusion.

In conclusion, multimodality molecular imaging and registration techniques in longitudinal studies will further advance our knowledge of the biological processes underlying bone remodeling, the onset and progression of diseases, and their treatment.

Conflict of Interest

The authors declare no conflict of interest.

ACKNOWLEDGMENTS

We gratefully acknowledge funding from the European Union (VPHOP FP7-ICT2008-223865).

References

1. Weinans H, Prendergast PJ, McNamara LM, Van der Linde JC. Stress-concentrating effect of resorption lacunae in trabecular bone. *J Biomech* 2006;**39**:734–741.
2. Huiskes R, Ruimerman R, van Lenthe GH, Janssen JD. Effects of mechanical forces on maintenance and adaptation of form in trabecular bone. *Nature* 2000;**405**:704–706.
3. Kurokawa K. How is plasma calcium held constant? Milieu interieur of calcium. *Kidney Int* 1996;**49**:1760–1764.
4. Jergas M, Genant HK. Current methods and recent advances in the diagnosis of osteoporosis. *Arthritis Rheum* 1993;**36**:1649–1662.
5. Ström O, Borgström F, Kanis JA, Compston J, Cooper C, McCloskey EV *et al.* Osteoporosis: burden, health care provision and opportunities in the EU. *Arch Osteoporos* 2011;**6**:59–155.
6. Kanis JA, Borgstrom F, De Laet C, Johansson H, Johnell O, Jonsson B *et al.* Assessment of fracture risk. *Osteoporos Int* 2005;**16**:581–589.
7. Reginster JY, Sarlet N, Lecart MP. Fractures in osteoporosis: the challenge for the new millennium. *Osteoporos Int* 2005;**16** (Suppl 1): S1–S3.
8. Kozloff KM, Quinti L, Patntirapong S, Hauschka PV, Tung CH, Weissleder R *et al.* Non-invasive optical detection of cathepsin K-mediated fluorescence reveals osteoclast activity *in vitro* and *in vivo*. *Bone* 2009;**44**:190–198.
9. Mayer-Kuckuk P, Boskey AL. Molecular imaging promotes progress in orthopedic research. *Bone* 2006;**39**:965–977.
10. Weissleder R, Mahmood U. Molecular imaging. *Radiology* 2001;**219**:316–333.
11. Rudin M, Weissleder R. Molecular imaging in drug discovery and development. *Nat Rev Drug Discov* 2003;**2**:123–131.
12. Weissleder R, Ntziachristos V. Shedding light onto live molecular targets. *Nat Med* 2003;**9**: 123–128.
13. Rahmim A, Zaidi H. PET versus SPECT: strengths, limitations and challenges. *Nucl Med Commun* 2008;**29**:193–207.
14. Rice BW, Cable MD, Nelson MB. *In vivo* imaging of light-emitting probes. *J Biomed Opt* 2001;**6**:432–440.
15. Ntziachristos V, Tung CH, Bremer C, Weissleder R. Fluorescence molecular tomography resolves protease activity *in vivo*. *Nat Med* 2002;**8**:757–760.
16. Contag CH, Bachmann MH. Advances in *in vivo* bioluminescence imaging of gene expression. *Annu Rev Biomed Eng* 2002;**4**:235–260.
17. Hounsfield GN. Computerized transverse axial scanning (tomography). 1. Description of system. *Br J Radiol* 1973;**46**:1016–1022.
18. Basilion JP, Yeon S, Botnar R. Magnetic resonance imaging: utility as a molecular imaging modality. *Curr Top Dev Biol* 2005;**70**:1–33.
19. Cherry SR. Multimodality *in vivo* imaging systems: twice the power or double the trouble? *Annu Rev Biomed Eng* 2006;**8**:35–62.
20. Townsend DW. Dual-modality imaging: combining anatomy and function. *J Nucl Med* 2008;**49**:938–955.
21. Hasegawa BH, Iwata K, Wong KH, Wu MC, Da Silva AJ, Tang HR *et al.* Dual-modality imaging of function and physiology. *Acad Radiol* 2002;**9**:1305–1321.
22. Beyer T, Townsend DW, Brun T, Kinahan PE, Charron M, Roddy R *et al.* A combined PET/CT scanner for clinical oncology. *J Nucl Med* 2000;**41**:1369–1379.
23. Buck AK, Nekolla S, Ziegler S, Beer A, Krause BJ, Herrmann K *et al.* Spect/Ct. *J Nucl Med* 2008;**49**:1305–1319.
24. Shao Y, Cherry SR, Farahani K, Meadors K, Siegel S, Silverman RW *et al.* Simultaneous PET and MR imaging. *Phys Med Biol* 1997;**42**:1965–1970.
25. Takahashi K, Inadama N, Murayama H, Yamaya T, Yoshida E, Nishikido F. Preliminary study of a DOI-PET detector with optical imaging capability. *IEEE Nuclear Science Symposium Conference Record* 2007;**5**:3318–3321.
26. Hyde D, de Kleine R, MacLaurin SA, Miller E, Brooks DH, Krucker T *et al.* Hybrid FMT-CT imaging of amyloid-beta plaques in a murine Alzheimer's disease model. *Neuroimage* 2009;**44**:1304–1311.
27. Stuker F, Baltes C, Dikaiou K, Vats D, Carrara L, Charbon E *et al.* Hybrid small animal imaging system combining magnetic resonance imaging with fluorescence tomography using single photon avalanche diode detectors. *IEEE Trans Med Imaging* 2011;**30**:1265–1273.
28. Hill DL, Batchelor PG, Holden M, Hawkes DJ. Medical image registration. *Phys Med Biol* 2001;**46**:R1–R45.
29. Beattie BJ, Forster GJ, Govantes R, Le CH, Longo VA, Zanzonico PB *et al.* Multimodality registration without a dedicated multimodality scanner. *Mol Imaging* 2007;**6**:108–120.
30. Chow PL, Stout DB, Komisopoulou E, Chatziioannou AF. A method of image registration for small animal, multi-modality imaging. *Phys Med Biol* 2006;**51**:379–390.
31. Russell RGG, Watts NB, Ebetino FH, Rogers MJ. Mechanisms of action of bisphosphonates: similarities and differences and their potential influence on clinical efficacy. *Osteoporos Int* 2008;**19**:733–759.
32. Moore AEB, Blake GM, Fogelman I. Quantitative measurements of bone remodeling using ^{99m}Tc-methylene diphosphonate bone scans and blood sampling. *J Nucl Med* 2008;**49**: 375–382.
33. Souris JS. Seeing the light in bone metabolism imaging. *Trends Biotechnol* 2002;**20**:364–366.
34. Hawkins RA, Choi Y, Huang SC, Hoh CK, Dahlbom M, Schiepers C *et al.* Evaluation of the skeletal kinetics of fluorine-18-fluoride ion with PET. *J Nucl Med* 1992;**33**:633–642.
35. Toegel S, Hoffmann O, Wadsak W, Ettlinger D, Mien LK, Wiesner K *et al.* Uptake of bone-seekers is solely associated with mineralisation! A study with ^{99m}Tc-MDP, ^{153}Sm-EDTMP and ^{18}F-fluoride on osteoblasts. *Eur J Nucl Med Mol Imaging* 2006;**33**:491–494.
36. Li J, Miller MA, Hutchins GD, Burr DB. Imaging bone microdamage *in vivo* with positron emission tomography. *Bone* 2005;**37**:819–824.
37. Messa C, Goodman WG, Hoh CK, Choi Y, Nissenson AR, Salusky IB *et al.* Bone metabolic activity measured with positron emission tomography and [^{18}F]fluoride ion in renal osteodystrophy: correlation with bone histomorphometry. *J Clin Endocrinol Metab* 1993;**77**: 949–955.
38. Hsu WK, Feeley BT, Krenek L, Stout DB, Chatziioannou AF, Lieberman JR. The use of ^{18}F-fluoride and ^{18}F-FDG PET scans to assess fracture healing in a rat femur model. *Eur J Nucl Med Mol Imaging* 2007;**34**:1291–1301.
39. Temmerman OP, Raijmakers PG, Heyligers IC, Comans EF, Lubberink M, Teule GJ *et al.* Bone metabolism after total hip revision surgery with impacted grafting: evaluation using $H_2{}^{15}O$ and [^{18}F]fluoride PET; a pilot study. *Mol Imaging Biol* 2008;**10**:288–293.
40. Ullmark G, Sorensen J, Langstrom B, Nilsson O. Bone regeneration 6 years after impaction bone grafting: a PET analysis. *Acta Orthop* 2007;**78**:201–205.
41. Grant FD, Fahey FH, Packard AB, Davis RT, Alavi A, Treves ST. Skeletal PET with ^{18}F-fluoride: applying new technology to an old tracer. *J Nucl Med* 2008;**49**:68–78.
42. Even-Sapir E, Metser U, Mishani E, Lievshitz G, Lerman H, Leibovitch I. The detection of bone metastases in patients with high-risk prostate cancer: ^{99m}Tc-MDP Planar bone scintigraphy, single- and multi-field-of-view SPECT, ^{18}F-fluoride PET, and ^{18}F-fluoride PET/CT. *J Nucl Med* 2006;**47**:287–297.
43. Zaheer A, Lenkinski RE, Mahmood A, Jones AG, Cantley LC, Frangioni JV. *In vivo* near-infrared fluorescence imaging of osteoblastic activity. *Nat Biotechnol* 2001;**19**:1148–1154.
44. Kozloff KM, Weissleder R, Mahmood U. Noninvasive optical detection of bone mineral. *J Bone Miner Res* 2007;**22**:1208–1216.
45. Mizrahi DM, Ziv-Polat O, Perlstein B, Gluz E, Margel S. Synthesis, fluorescence and biodistribution of a bone-targeted near-infrared conjugate. *Eur J Med Chem* 2011;**46**: 5175–5183.
46. Kovar JL, Xu XS, Draney D, Cupp A, Simpson MA, Olive DM. Near-infrared-labeled tetracycline derivative is an effective marker of bone deposition in mice. *Anal Biochem* 2011;**416**:167–173.
47. Lian JB, Stein GS, Stein JL, van Wijnen AJ. Osteocalcin gene promoter: unlocking the secrets for regulation of osteoblast growth and differentiation. *J Cell Biochem Suppl* 1998; **30–31**:62–72.
48. Boskey AL, Gadaleta S, Gundberg C, Doty SB, Ducy P, Karsenty G. Fourier transform infrared microspectroscopic analysis of bones of osteocalcin-deficient mice provides insight into the function of osteocalcin. *Bone* 1998;**23**:187–196.

49. Clemens TL, Tang H, Maeda S, Kesterson RA, Demayo F, Pike JW *et al.* Analysis of osteocalcin expression in transgenic mice reveals a species difference in vitamin D regulation of mouse and human osteocalcin genes. *J Bone Miner Res* 1997;**12**:1570–1576.
50. Iris B, Zilberman Y, Zeira E, Galun E, Honigman A, Turgeman G *et al.* Molecular imaging of the skeleton: quantitative real-time bioluminescence monitoring gene expression in bone repair and development. *J Bone Miner Res* 2003;**18**:570–578.
51. Barry FP, Murphy JM. Mesenchymal stem cells: clinical applications and biological characterization. *Int J Biochem Cell Biol* 2004;**36**:568–584.
52. Degano IR, Vilalta M, Bago JR, Matthies AM, Hubbell JA, Dimitriou H *et al.* Bioluminescence imaging of calvarial bone repair using bone marrow and adipose tissue-derived mesenchymal stem cells. *Biomaterials* 2008;**29**:427–437.
53. Wetterwald A, van der Pluijm G, Que I, Sijmons B, Buijs J, Karperien M *et al.* Optical imaging of cancer metastasis to bone marrow: a mouse model of minimal residual disease. *Am J Pathol* 2002;**160**:1143–1153.
54. Kozloff KM, Quinti L, Tung C, Weissleder R, Mahmood U. Non-invasive imaging of osteoclast activity via near-infrared cathepsin-K activatable optical probe. *J Musculoskelet Neuronal Interact* 2006;**6**:353.
55. Schulte FA, Lambers FM, Kuhn G, Müller R. *In vivo* micro-computed tomography allows direct three-dimensional quantification of both bone formation and bone resorption parameters using time-lapsed imaging. *Bone* 2011;**48**:433–442.
56. Lambers FM, Schulte FA, Kuhn G, Webster DJ, Müller R. Mouse tail vertebrae adapt to cyclic mechanical loading by increasing bone formation rate and decreasing bone resorption rate as shown by time-lapsed *in vivo* imaging of dynamic bone morphometry. *Bone* 2011;**49**: 1340–1350.
57. Roshan-Ghias A, Lambers FM, Gholam-Rezaee M, Müller R, Pioletti DP. *In vivo* loading increases mechanical properties of scaffold by affecting bone formation and bone resorption rates. *Bone* 2011;**49**:1357–1364.
58. Dotan ZA. Bone imaging in prostate cancer. *Nat Clin Pract Urol* 2008;**5**:434–444.
59. Coleman RE. Clinical features of metastatic bone disease and risk of skeletal morbidity. *Clin Cancer Res* 2006;**12**:6243s–6249s.
60. Coleman RE. Metastatic bone disease: clinical features, pathophysiology and treatment strategies. *Cancer Treat Rev* 2001;**27**:165–176.
61. Chen YW, Huang MY, Hsieh JS, Hou MF, Chou SH, Lin CL. Discordant findings of skeletal metastasis between Tc^{99M} MDP bone scans and F^{18} FDG PET/CT imaging for advanced breast and lung cancers—two case reports and literature review. *Kaohsiung J Med Sci* 2007;**23**: 639–646.
62. Kumar J, Seith A, Kumar A, Sharma R, Bakhshi S, Kumar R *et al.* Whole-body MR imaging with the use of parallel imaging for detection of skeletal metastases in pediatric patients with small-cell neoplasms: comparison with skeletal scintigraphy and FDG PET/CT. *Pediatr Radiol* 2008;**38**:953–962.
63. Taira AV, Herfkens RJ, Gambhir SS, Quon A. Detection of bone metastases: assessment of integrated FDG PET/CT imaging. *Radiology* 2007;**243**:204–211.
64. Strobel K, Exner UE, Stumpe KD, Hany TF, Bode B, Mende K *et al.* The additional value of CT images interpretation in the differential diagnosis of benign vs malignant primary bone lesions with 18F-FDG-PET/CT. *Eur J Nucl Med Mol Imaging* 2008;**35**:2000–2008.
65. Winkelmann CT, Figueroa SD, Rold TL, Volkert WA, Hoffman TJ. Microimaging characterization of a B16-F10 melanoma metastasis mouse model. *Mol Imaging* 2006;**5**:105–114.
66. Kim MR, Roh JL, Kim JS, Choi SH, Nam SY, Kim SY. ^{18}F-fluorodeoxyglucose-positron emission tomography and bone scintigraphy for detecting bone metastases in patients with malignancies of the upper aerodigestive tract. *Oral Oncol* 2008;**44**:148–152.
67. Berger F, Lee YP, Loening AM, Chatziioannou A, Freedland SJ, Leahy R *et al.* Whole-body skeletal imaging in mice utilizing microPET: optimization of reproducibility and applications in animal models of bone disease. *Eur J Nucl Med Mol Imaging* 2002;**29**:1225–1236.
68. Fritz V, Louis-Plence P, Apparailly F, Noel D, Voide R, Pillon A *et al.* Micro-CT combined with bioluminescence imaging: a dynamic approach to detect early tumor-bone interaction in a tumor osteolysis murine model. *Bone* 2007;**40**:1032–1040.
69. Silva MJ, Uthgenannt BA, Rutlin JR, Wohl GR, Lewis JS, Welch MJ. *In vivo* skeletal imaging of 18F-fluoride with positron emission tomography reveals damage- and time-dependent responses to fatigue loading in the rat ulna. *Bone* 2006;**39**:229–236.
70. Einhorn TA. Enhancement of fracture-healing. *J Bone Joint Surg Am* 1995;**77**:940–956.
71. Zlowodzki M, Obremskey WT, Thomison JB, Kregor PJ. Functional outcome after treatment of lower-extremity nonunions. *J Trauma* 2005;**58**:312–317.
72. O'Loughlin PF, Morr S, Bogunovic L, Kim AD, Park B, Lane JM. Selection and development o f preclinical models in fracture-healing research. *J Bone Joint Surg Am* 2008;**90** (Suppl 1): 79–84.
73. Lankinen P, Makinen TJ, Poyhonen TA, Virsu P, Salomaki S, Hakanen AJ *et al.* (68)Ga-DOTAVAP-P1 PET imaging capable of demonstrating the phase of inflammation in healing bones and the progress of infection in osteomyelitic bones. *Eur J Nucl Med Mol Imaging* 2008;**35**:352–364.
74. Lee SW, Padmanabhan P, Ray P, Gambhir SS, Doyle T, Contag C *et al.* Stem cell-mediated accelerated bone healing observed with *in vivo* molecular and small animal imaging technologies in a model of skeletal injury. *J Orthop Res* 2009;**27**:295–302.
75. Zilberman Y, Kallai I, Gafni Y, Pelled G, Kossodo S, Yared W *et al.* Fluorescence molecular tomography enables *in vivo* visualization and quantification of nonunion fracture repair induced by genetically engineered mesenchymal stem cells. *J Orthop Res* 2008;**26**:522–530.
76. Oskouian RJ, Pelled G, Zilberman Y, Tal Y, Gazit Z, Gazit D. Novel, injectable, genetically engineered stem cell-based system for anterior spinal fusion. *Mol Ther* (Conference abstract). 2006;**13**:S173–S174.
77. Young H, Baum R, Cremerius U, Herholz K, Hoekstra O, Lammertsma AA *et al.* Measurement of clinical and subclinical tumour response using [^{18}F]-fluorodeoxyglucose and positron emission tomography: review and 1999 EORTC recommendations. European Organization for Research and Treatment of Cancer (EORTC) PET Study Group. *Eur J Cancer* 1999;**35**:1773–1782.
78. Krug R, Carballido-Gamio J, Banerjee S, Stahl R, Carvajal L, Xu D *et al. In vivo* bone and cartilage MRI using fully-balanced steady-state free-precession at 7 tesla. *Magn Reson Med* 2007;**58**:1294–1298.